LARGE-SCALE STRUCTURES OF A NATURAL-CONVECTION BOUNDARY LAYER CAPTURED WITH A PIV TECHNIQUE

Yasuo Hattori
Fluid Science Department, Central Research Institute of Electric Power Industry
1646 Abiko, Abiko-shi, Chiba 270-1194, Japan, yhattori@criepi.denken.or.jp

Toshihiro Tsuji
Department of Environmental Technology, Graduate School of Engineering, Nagoya Institute of Technology
Gokiso-cho, Showa-ku, Nagoya 466-8555, Japan, tsuji@megw.mech.nitech.ac.jp

Yasutaka Nagano
Department of Mechanical Engineering, Nagoya Institute of Technology
Gokiso-cho, Showa-ku, Nagoya 466-8555, Japan, nagano@heat.mech.nitech.ac.jp

Nobukazu Tanaka
Fluid Science Department, Central Research Institute of Electric Power Industry
1646 Abiko, Abiko-shi, Chiba 270-1194, Japan, n-tanaka@criepi.denken.or.jp

ABSTRACT

The characteristics of large-scale structures in the outer layer of the natural-convection boundary layer have been experimentally investigated. The special attention is paid to the interrelation between the large-scale structures and the turbulence production. The measured two-dimensional velocity vectors with a PIV (particle image velocimetry) show that the structures in the outer layer of natural convection are strikingly different from those in forced convection, while the structures in natural and forced convection are similar near the maximum mean velocity location. In the outer layer, it is observed that the winding of high momentum flows generates strong vorticies with scales beyond the boundary layer thickness in the x direction, and the important 'Q1 (u>0, v>0)' and 'Q3 (u<0, v<0)' motions contributing to the Reynolds stress $\overline{uv}$ are frequently observed. Such fluid motions are related directly to the turbulence generation in the outer layer of the boundary layer and cause the non-uniformity of the velocity field. As a result, the cross-correlation between the instantaneous Reynolds shear stress and velocity gradient takes a negative value at the maximum mean velocity location, though the product of relevant mean values becomes zero. Thus, the peculiar profile of $\overline{uv}$ occurs near the maximum mean velocity location.

INTRODUCTION

The large-scale structures in the outer region of wall turbulent shear flows, which play an important role in turbulent transport, have already been investigated extensively. However, most of them are concerned chiefly with forced-convection boundary layers, and researches on natural convection have been insufficient. In fact, there are only few investigations on the structural characteristics in the outer layer of the turbulent natural-convection boundary layer along a vertical heated plate, which is one of the typical buoyant flows. Here, the outer layer of the natural-convection boundary layer corresponds to the area from the maximum velocity location to the edge of the boundary layer. Cheesewright and Doan (1978) and Cheesewright and Dastbaz (1983) conducted simultaneous measurements at two points in the thermal field with thermocouples. The spatial and temporal correlations in the thermal field were examined, and they found that the decay of the maximum correlations (the memory of turbulence) in the thermal field was similar to that observed in usual forced-convection boundary layers. Moreover, it was found from the distribution of the spatial correlations that the convection velocities are greater than the local mean velocity. Kitamura et al. (1985) performed visualizations of the wall temperature and the velocity field with water and air as the working fluids under the uniform heat-flux conditions, and suggested that the large eddy motions closely correlate to the turbulent transport in the natural-convection boundary layer. Tsuji et al. (1992) carried out the measurement of instantaneous temperature profiles and simultaneous measurements of velocity and temperature at two points in the boundary layer by using a thermocouple rake and a pair of hot-wire/cold-wire arrangements, and discussed the temporal variation of the thermal field and the space-time correlation coefficients of temperature and velocity fluctuations. The characteristic length scales of velocity and temperature fluctuations were also obtained. Through these experiments, the turbulence structure in the thermal field has been clarified to some extent. However, the details of the turbulence structure in the velocity field have not been fully understood, because of the difficulty in obtaining the multipoint simultaneous velocities.

On the other hand, the credible experimental data for turbulent statistics of the natural-convection boundary layer have been accumulated by Tsuji and Nagano (1988a, 1988b). Consequently, it is revealed that the turbulent characteristics of natural convection essentially differ from

those of forced convection, e.g., the mean value of Reynolds shear stress $\overline{uv}$ is not necessarily zero but almost positive at the maximum mean velocity location, despite the zero velocity gradient; the intensity of velocity fluctuations becomes maximum in the outer layer, while the maximum intensity of temperature fluctuations occurs in the inner layer from the wall to the maximum velocity location. These results imply that the turbulent energy production in the natural-convection boundary layer may be controlled by the peculiar mechanism. Thus, the detailed information on the turbulence structure in the natural-convection boundary layer has been eagerly awaited to comprehend the turbulence generation mechanism.

The present study aims at clarifying the structural characteristics of large-scale fluid motions in the outer layer of the natural-convection boundary layer along a vertical heated plate. The special attention is paid to the interrelation between the large-scale structures and the turbulence production. Two-dimensional velocity vectors in the boundary layer are measured with a particle image velocimetry (PIV). Through the spatial correlations and velocity vectors, the spatial structures in the velocity field are investigated closely. Then, the relationship between the large-scale structures and the peculiar turbulent characteristics of the natural-convection boundary layer is also discussed.

EXPERIMENTAL APPARATUS AND PROCEDURE

The experimental apparatus used in the present study was designed to be applicable to the experiments for natural-, combined- and forced-convection boundary layers, and has been mainly used to examine the combined-convection boundary layer. Since the details of the apparatus were described in our previous papers (Hattori et al., 2000, 2001), the specifications only for the pure natural-convection experiment are mentioned as follows. The heated surface generating a buoyant flow was a 4 m high and 0.8 m wide aluminum plate, and had a mirror finish to reduce the heat loss by radiation. The surface temperature, which was monitored with forty-eight thermocouples embedded in the plate, was kept uniform by controlling the heating current of split heaters attached to the backside of the plate. The heated plate was placed vertically in the test section (1×1 m^2 in area and 6.2 m high) of the vertical wind tunnel with solid boundaries. The whole test section was coated with a thick layer of heat insulating material to curb the effect of change in the ambient temperature on the boundary layer flow.

Defining the coordinates x, y and z as being the streamwise, transverse and spanwise directions, respectively, the flow fields in the (x-y) plane perpendicular to the heated plate and in the (x-z) plane parallel to the flat plate were visualized, and the two-dimensional velocity vectors were measured with a PIV. The boundary layer flow seeded with olive-oil mists were illuminated by a double-pulsed Nd:YAG laser system (New Wave 90 mJ/pulse) with the laser sheet thickness of about 2 mm. The time intervals between two-pulsed illuminations were set at 400 and 500 μs for the measurements in the (x-y) and (x-z) planes, respectively. Particle-containing flow images were captured by a CCD camera (Kodak MEGA-PLUS ES1.0). The camera lens of an 85 mm focal length was used to reduce the influence of out-of-plane velocity components. The distances between the image recording plane of the CCD camera and the illuminating laser sheet were approximately 720 mm for the (x-y) plane measurement and 1,100 mm for the (x-z) plane measurement, and the physical sizes of the measuring areas in the (x-y) and (x-z) planes were 72.0×70.9 mm^2 (=0.66δ×0.67δ) and 110.0×108.3 mm^2 (=$1.0\delta \times 1.0\delta$), respectively. Here, δ denotes the integral thickness of the velocity boundary layer (Tsuji and Nagano, 1989). The captured images were directly stored in a hard disk on PC as bmp files at 10 fps.

The velocity vectors were calculated by using a cross-correlation method. The sizes of the interrogation windows were 2.2×2.2 mm^2 and 3.4×3.4 mm^2 for the measurements in the (x-y) and (x-z) planes, respectively. The sub-pixel algorithm on the assumption of a Gaussian profile for the spatial correlation was also applied to improve the dynamic spatial range of velocity vectors. After the calculation of local displacements of particle images, incorrect vectors were removed with a median filter (Raffel et al., 1998), and empty data cells were filled with interpolated velocity vectors. Then, the statistical analysis was performed by averaging over 1,000 PIV images in both (x-y) and (x-z) planes.

It was confirmed in a preliminary experiment on the natural-convection boundary layer that low frequency fluctuations dominant in the boundary layer were well captured with the PIV and the measured results for the mean velocity, the intensities of velocity fluctuations and the Reynolds shear stress agree well with the hot- and cold-wire measurements (Hattori et al., 2001). Thus, it was expected that the PIV definitely provided useful information about comparatively large-scale fluid motions in the outer layer of the natural-convection boundary layer.

The experiments were conducted under the conditions of the isothermal wall temperature T_w = 90 ℃ and the ambient fluid temperature T_∞ = 20～25 ℃. The measuring location was fixed at the vertical distance x = 2.965 m from the leading edge of the flat plate. Physical properties were evaluated at the film temperature T_f [= $(T_w+T_\infty)/2$] except for the coefficient of volume expansion β, and the local Grashof number Grx [= $g\beta(T_w-T_\infty)x^3/\nu^2$; ν is the kinematic viscosity] equaled to 1.60～1.77×10^{11}.

RESULTS AND DISCUSSION

Two-point spatial correlation

Contours of the two-point correlation coefficients for the streamwise velocity fluctuation u and the transverse velocity fluctuation v in the (x-y) plane are plotted in Figs. 1 and 2, respectively. The fixed points y_{ref} (at x = 2.965 m) to calculate spatial-correlation coefficients are set at the maximum mean velocity location (y_{ref}/δ = 0.1) and at the location in the outer layer (y_{ref}/δ = 0.37). At y_{ref}/δ = 0.1, the correlation contour for u fluctuation is elongated in the x direction and is inclined at a small angle to the wall. The inclination of contour defined as the angle between the ridgeline and the wall has been used to define the orientation of dominant flow structures. The average angle estimated from the contour shown in Fig. 1(a) is 7°, and this value is approximately identical to that for forced convection (Liu et al., 2001). On the other hand, it was

reported that the contour of spatial-correlation coefficients for temperature fluctuation in the thermal field of natural convection had a different value of inclination (=15°～20°) (Cheesewright and Dastbaz, 1983). This fact indicates a poor relation between the structures in the velocity and thermal fields of the natural-convection boundary layer. As shown in Fig. 1(a), high values of correlation coefficients for u fluctuation also appear in the inner layer. This implies that the large-scale fluid motions have an effect on the structure very near the wall. In contrast to u fluctuation, the contour of correlation coefficient for v fluctuation shown in Fig. 2(a) rapidly shrinks with an increase in the spacing between two points, especially in the near-wall region. The shapes of these contours are close to what was observed in the forced-convection boundary layer. Thus, near the maximum mean velocity location in natural convection, the structure of the velocity field seems to be fairly similar to that for forced convection. However, for the correlations for u and v fluctuations in the outer layer, there exists a noticeable discrepancy between natural and forced convection (Liu et al., 2001). The region showing high positive correlations for u fluctuation expands when the fixed point moves away from the near-wall as shown Fig. 1(b). At $y_{ref}/\delta =$ 0.37, the streamwise scale of the contour of the correlation coefficient lager than 0.6 (Nakagawa and Hanratty, 2001) exceeds the integral thickness of the boundary layer δ. The correlation contour for v fluctuation also expands when the fixed-point moves away from the near-wall as shown in Fig. 2(b), but the contour rounds in contrast to the elongated contour for u fluctuation. Such contours of correlation coefficients corresponding to the large-scale structure of the velocity field in the outer layer are somewhat different from those observed in the forced-convection boundary layer (Liu et al., 2001), e.g., the correlation contour for u fluctuation in natural convection takes a inclination opposite to forced convection, because the fluid velocity reduces toward the edge of the boundary layer.

Figure 3 shows the contour of spatial correlation coefficients for u fluctuation in the (x-z) plane (y_{ref}/δ=0.1). This contour is significantly different from that for forced convection (Abe et al, 2002), i.e., the correlation contour for u fluctuation in the outer layer of natural convection becomes positive in the whole visualized region ($1.0\delta \times 1.0\delta$), while that for forced convection alters from positive to negative as the spacing between two points in the z direction increases. Thus, the streaky structure as observed in forced convection is not clearly detected in the natural-convection boundary layer.

Dynamical characteristics

An example of fluctuating velocity vectors in the (x-y) plane is presented in Fig. 4. The gray levels indicating instantaneous value of $-uv(\partial U/\partial y)$, which represents the generation of turbulent kinetic energy due to instantaneous Reynolds shear stress and velocity gradient, and vorticity ω_z are also displayed in the figure. These quantities are normalized by the maximum mean velocity $\overline{U}_m$ and the integral thickness of velocity boundary layer δ. It is observed in Fig.4 that the winding of high momentum flows generates strong vorticies with scales beyond the thickness δ in the x direction. Also observed is the large-scale fluid moving at a high-speed from the maximum mean velocity location toward the outer layer, which is the important 'Q1 (u>0, v>0)' motion contributing to the Reynolds shear stress. Simultaneously, the 'Q3 (u<0, v<0)' motion of lower-speed fluid sifting toward the wall appears near the location where the Q1 motion arises. Such fluid motions cause large positive values of $-uv(\partial U/\partial y)$, because the instantaneous velocity gradient becomes negative at high rates in the outer layer. Thus, it is confirmed that the large-scale structures involving the Q1 and Q3 motions are directly related to the turbulence generation in the outer layer of the natural-convection boundary layer.

The choice of the reference frame is important to identify vortex structures with PIV (Adrian et al., 2000). Then, the fluctuating velocity fields calculated with the convection velocities $\overline{U}_c = 0.4\overline{U}_m$, $0.6\overline{U}_m$ and $0.8\overline{U}_m$, are presented in Fig. 5, compared with the velocity field obtained with a Reynolds decomposition. At $\overline{U}_c = 0.8\overline{U}_m$, the vortex structures are clearly observed, and it is found that the convection velocity $\overline{U}_c$ exceeds the local mean velocity in the outer layer. This result correlates well with that obtained by the spatio-temporal measurement for the thermal field (Cheesewright and Dastbaz, 1983; Tsuji et al., 1992).

A time series of fluctuating velocity vectors measured with $\overline{U}_c = 0.8\overline{U}_m$ is shown in Fig. 6, normalized with the maximum mean velocity $\overline{U}_m$. Corresponding to the winding of the velocity field, vortices are generated through the strong shear layer. Simultaneously, the uniform momentum zones (Adrian, 2001) locally appear with low- and high-speed fluid motions and the non-uniformity of the velocity field becomes significant in both x and y as shown in Fig.6(d). Then, a large-scale Q1 motion appears in the whole visualized region ($1.0\delta \times 1.0\delta$). Such phenomena cause a large fluctuation of the maximum velocity location y_{Um} where instantaneous streamwise velocity takes a maximum value. Figure 7 demonstrates time traces of y_{Um} and the instantaneous maximum velocity U_m. The skewness factor of y_{Um} becomes positive and the flatness factor of y_{Um} is significantly larger than the value of 3. So that, the probability density function of y_{Um} is slightly skewed negative and y_{Um} shows highly intermittent behavior.

The cross-correlation coefficient between the instantaneous Reynolds shear stress and velocity gradient is presented in Fig. 8. The correlation coefficient at the maximum mean velocity location takes a negative value, whereas the product of relevant mean values becomes zero. This fact suggests that the turbulence structure in the outer layer is closely connected with the peculiar behavior of the Reynolds shear stress in the natural-convection boundary layer. Thus, it may be difficult to correctly predict such a behavior appeared in the turbulent natural-convection boundary layer by using turbulence models based on a Reynolds decomposition.

Conditional sampling

The effects of instantaneous velocity gradient $\partial U/\partial y$ at the maximum mean velocity location on the two-point spatial correlation coefficients for velocity fluctuations were examined to understand the characteristics of large-

scale fluid motions in the outer layer more minutely. The contours of spatial correlation coefficients for u and v fluctuations in the (x-y) plane are shown in Figs. 9 and 10, respectively. The fixed point y_{ref} is set at the maximum mean velocity location ($y_{ref}/\delta = 0.1$). The feature of correlation contour for v fluctuation appreciably changes with the sign of $\partial U/\partial y$, while the shape of correlation contour for u fluctuation is quite independent of the sign of $\partial U/\partial y$. The correlated region for $\partial U/\partial y > 0$, which may connect with the Q1 motion, becomes noticeably narrower than that obtained for $\partial U/\partial y < 0$, which may correspond to the Q3 motion. In particular, the correlation coefficient in the y direction drastically decreases. The profiles of streamwise and transverse mean velocities, $\overline{U}$ and $\overline{V}$, and the Reynolds shear stress $\overline{uv}$ obtained for $\partial U/\partial y > 0$ and $\partial U/\partial y < 0$ are shown in Figs. 11, and 12, respectively. These quantities are normalized by the maximum mean velocity $\overline{U}_m$. When $\partial U/\partial y$ takes negative values, the maximum mean velocity location approaches the wall and the value of $\overline{V}$ is negative. Simultaneously, the positive values of $\overline{uv}$ become larger. On the contrary, when $\partial U/\partial y$ takes positive values, the maximum mean velocity location moves toward the outer layer, and the value of $\overline{V}$ becomes slightly positive. These results suggest that the scales of fluid motion for $\partial U/\partial y < 0$ is rather large compared with those for $\partial U/\partial y > 0$, and thus it is found that the peculiar $\overline{uv}$ profile near the maximum mean velocity location is increasingly caused by the large-scale motion (Q1 motion) for $\partial U/\partial y < 0$.

CONCLUDING REMARKS

The characteristics of large-scale structures in the outer layer of the natural-convection boundary layer were experimentally investigated, especially paying attention to the mechanism of turbulence generation. Two-dimensional velocity vectors were measured with a particle image velocimetry (PIV), and the structure in the velocity field was discussed in detail. The results of the present study may be summarized as follows:

1. The structure in the outer layer of natural convection is strikingly different from that in forced convection, while the structures of natural and forced convection are similar near the maximum mean velocity location.
2. The winding of high momentum flows generates strong vorticies with scales beyond the integral thickness of the boundary layer δ in the x direction. The important 'Q1 ($u>0$, $v>0$)' and 'Q3 ($u<0$, $v<0$)' motions contributing to the Reynolds shear stress are frequently observed in the outer layer, and it is confirmed that such fluid motions are directly related to the turbulence generation in the natural-convection boundary layer.
3. The cross-correlation coefficient between the instantaneous Reynolds shear stress and velocity gradient takes a negative value at the maximum mean velocity location, whereas the product of relevant mean values becomes zero.
4. The feature of correlation contour for v fluctuation appreciably changes with the sigh of instantaneous velocity gradient $\partial U/\partial y$, while the shape of correlation contour for u fluctuation is independent of the sign of $\partial U/\partial y$. The peculiar $\overline{uv}$ profile near the maximum mean velocity location is increasingly caused by the large-scale motion (Q1 motion) for $\partial U/\partial y < 0$.

REFERENCE

Abe, H., Matsuo, Y., and Kawamura, H., 2002, "An analysis of large-scale structures through DNS of turbulent heat transfer in a channel flow," *Proc. 16th CFD symp.*, E11-2, (*in Japanese*).

Adrian, R. J., Meinhart, C. D., and Tomkins, C. D., 2000, "Vortex organization in the outer region of the turbulent boundary layer," *J. Fluid Mech.*, vol. 422, pp. 1-54.

Cheesewright, R., and Doan, K. S., 1978, "Space-time correlation measurements in a turbulent natural convection boundary layer," *Int. J. Heat Mass Transfer*, vol. 21, pp. 911-921.

Cheesewright, R., and Dastbaz, A., 1983, "The structure of turbulence in a natural convection boundary layer," *Proc., 4th Turbulent Shear Flow Symp.*, 17.25-17.30.

Hattori, Y., Tsuji, T., Nagano Y., and Tanaka, N., 2000, "Characteristics of turbulent combined-convection boundary layer along a vertical heated plate," *Int. J. Heat Fluid Flow*, vol. 21, pp. 520-525.

Hattori, Y., 2001, "Turbulent characteristics and transition behavior of combined-convection boundary layer along a vertical heated plate," Ph.D. thesis, Nagoya Institute of Technology.

Kitamura, K., Koike, M., Fukuoka, I., and Saito, T., 1985, "Large eddy structure and heat transfer of turbulent natural convection along a vertical flat plate," *Int. J. Heat Mass Transfer*, vol. 28, pp. 837-850.

Liu, Z., Adrian, R. J., and Hanratty, T. J., 2001, "Large-scale modes of turbulent channel flow: transport and structure," *J. Fluid Mech.*, vol. 448, pp. 53-80.

Nakagawa, S., and Janratty, T. J., 2001, "Particle image velocimetry measurements of flow over a wavy wall," *Phys. of Fluids*, vol. 13, pp. 3504-3507.

Raffel, M., Willert, C., and Kompenhans, J., 1998, *Particle image velocimetry,* Springer-Verlag, Berlin.

Tsuji, T., and Nagano, Y., 1988a, "Characteristics of a turbulent natural convection boundary layer along a vertical flat plate," *Int. J. Heat Mass Transfer*, vol. 31, pp. 1723-1734.

Tsuji, T., and Nagano, Y., 1988b, "Turbulence measurements in a natural convection boundary layer along a vertical flat plate," *Int. J. Heat Mass Transfer*, vol. 31, pp. 2101-2111.

Tsuji, T., and Nagano, Y., 1989, "Velocity and temperature measurements in a natural convection boundary layer along a vertical flat plate," *Exp. Thermal Fluid Sci.*, vol. 2, pp. 208-215.

Tsuji, T., Nagano, Y., and Tagawa, M., 1992, "Experiment on spatio-temporal turbulent structures of a natural convection boundary layer," *ASME J. Heat Transfer*, vol. 114, pp. 901-908.

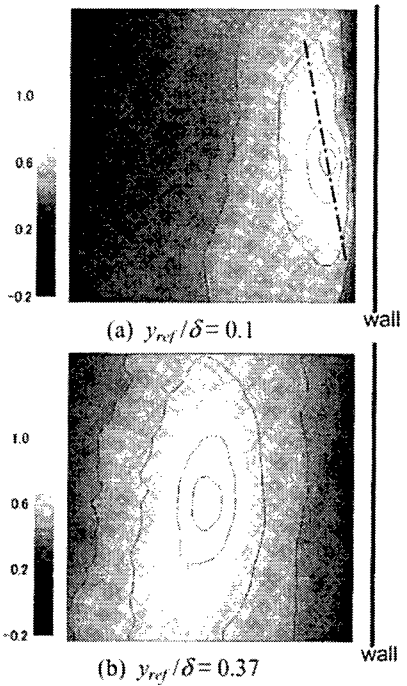

Fig. 1 Contour of spatial correlation coefficient for u fluctuation in (x-y) plane

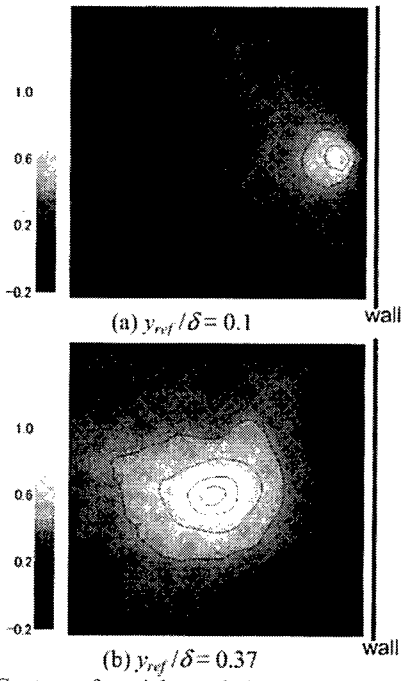

Fig. 2 Contour of spatial correlation coefficient for v fluctuation in (x-y) plane

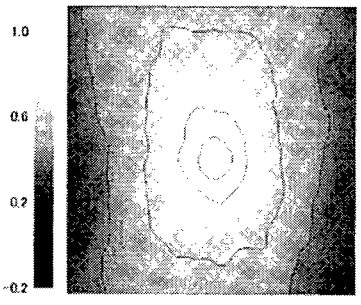

Fig. 3 Contour of spatial correlation coefficient for u fluctuation in (x-z) plane at $y_{ref}/\delta = 1.0$

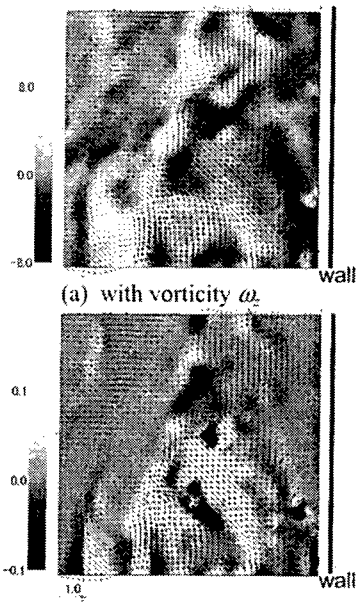

Fig. 4 Fluctuating velocity vectors in (x-y) plane

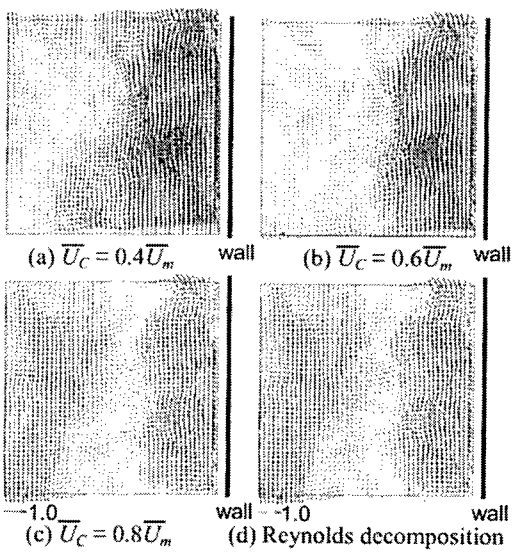

Fig. 5 Fluctuating velocity vectors

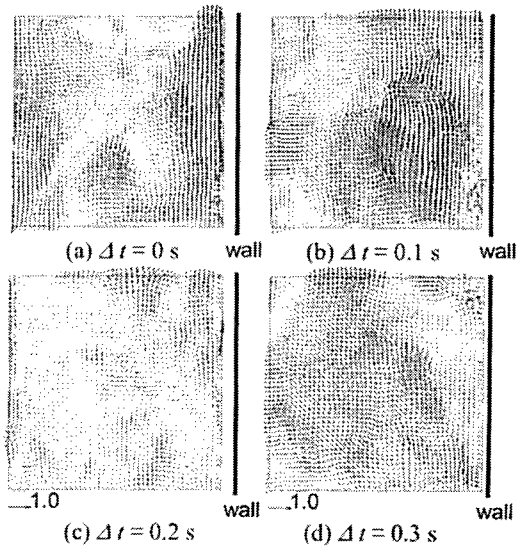

Fig. 6 Time series of fluctuating velocity vectors at $\overline{U_C} = 0.8\overline{U_m}$

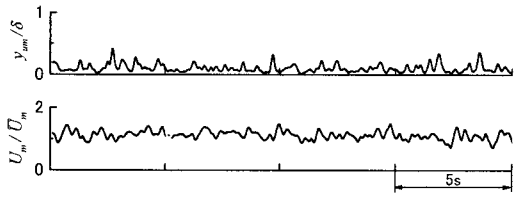

Fig. 7 Time traces of instantaneous maximum velocity and its location

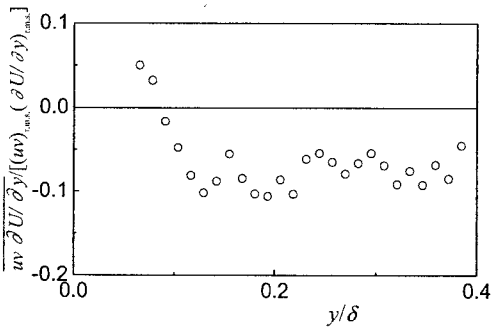

Fig. 8 Cross-correlation coefficient between instantaneous Reynolds shear stress and velocity gradient

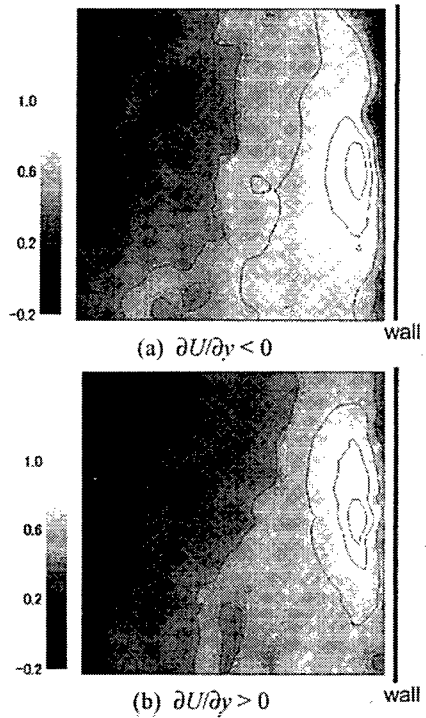

Fig. 9 Contour of spatial correlation coefficient for u fluctuation in (x-y) plane at $y_{ref}/\delta = 0.1$

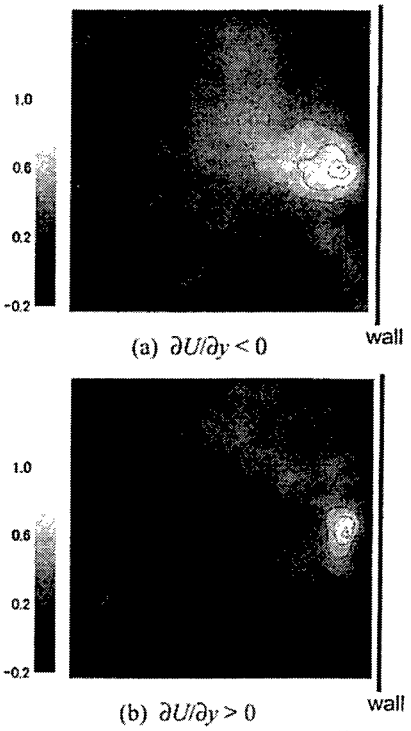

Fig. 10 Contour of spatial correlation coefficient for v fluctuation in (x-y) plane at $y_{ref}/\delta = 0.1$

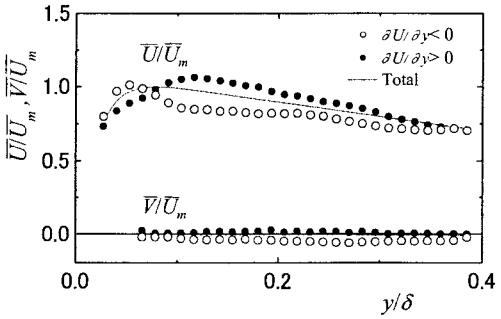

Fig. 11 Profiles of mean velocity

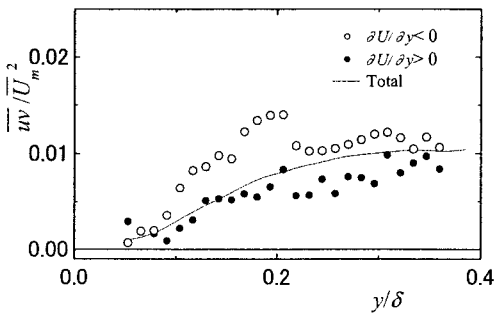

Fig. 12 Profiles of Reynolds shear stress